Audrius MALŪKAS[1*], Sergejus LEBEDEVAS[2]

ASSESSMENT OF HEAT BALANCE IN THE FSRU REGASIFICATION CYCLE ALIGNS WITH IMO'S DECARBONISATION STRATEGY

Summary. In 2023, the International Maritime Organization revised its greenhouse gas strategy, striving to reduce annual emissions from international shipping by at least 70% by 2040. The Mediterranean Sea will become an emission control area for sulphur oxides and particulate matter from May 2025, and the EU will include shipping in its Emission Trading System from 2024. Liquid natural gas is expected to become a cleaner marine fuel, but it alone cannot meet emission reduction goals. The cryogenic carbon capture process can separate CO_2 from exhaust gases, compress it, and store it in a liquid state with high density. This study aims to integrate an energy balance equation model to analyse the energy exchange in the regasification process and identify potential areas for improvement and targeted solutions to enhance performance and comply with IMO emission regulations. Based on a mathematical model, the energy balances are calculated and yield the following results: steam heater (26,999 kW), R-290 preheater (5,837 kW), trim heater (3,290 kW), R-290 evaporator (13,322 kW), and LNG vaporiser (23,118 kW). A report also determined that within a temperature range between -56.6°C and 31°C and a pressure range of greater than 5.2 bar (absolute) and less than 74 bar (absolute), the CO_2 is in a liquid phase. Due to CO_2 density which fluctuates in liquid at 1032 kg/m^3 and in solid phase at 1562 kg/m^3 the physical condition is compatible with the storage stage of capture emission.

1. INTRODUCTION

In 2023, the International Maritime Organization (IMO), which is leading efforts to decarbonise the shipping industry, adopted targets to reduce annual greenhouse gas emissions from international shipping by at least 70% by 2040. In addition to implementing emissions targets, IMO is leading a plan to introduce the Mediterranean Sea as an emission control area for sulphur oxides and particulate matter from May 2025. Moreover, the European Union (EU) will include shipping in its Emissions Trading Scheme from 2024 [1]. The urgent need to achieve climate goals and reduce carbon emissions has led to the implementation of various measures aimed at limiting the access of emissions to the atmosphere. Among these measures, two distinct approaches can be identified: financial liability and the strengthening of environmental requirements for the industrial and transport sectors. In particular, the current system imposes financial liability on industry, electricity producers and airlines for their emissions, thereby incentivising these entities to explore emission reduction options that translate into lower taxes: the EU Emissions Trading Scheme (EU ETS) [2].

As a fundamental component of the EU's climate change policy, the EU ETS is an indispensable tool for cost-effectively reducing greenhouse gas emissions. In 2023, the EU agreed to include shipping in the EU ETS, which will require ships over 5,000 GT carrying cargo or passengers for commercial purposes in the EU to purchase and surrender emission allowances for their CO_2 emissions from 2024

[1] Klaipeda University; H. Manto str. 84, LT-92294, Klaipėda, Lithuania; e-mail: malukasaudrius@gmail.com; orcid.ord/0009-0000-0700-0028

[2] Klaipeda University; H. Manto str. 84, LT-92294, Klaipėda, Lithuania; e-mail: sergejus.lebedevas@ku.lt; orcid.ord/0000-0002-4688-9568

[*] Corresponding author. E-mail: malukasaudrius@gmail.com

onwards. The inclusion of offshore vessels is planned for 2027. This update highlights the latest information on the EU ETS. Then, in 2022, the 79th session of the IMO's Marine Environment Protection Committee (MEPC 79) highlighted the agreement reached to adopt the Mediterranean Sea as a Sulphur Emission Control Area (SECA) from 1 May 2025 [3].

The measures established in place on the revision of the IMO GHG Strategy are expected to boost Liquified Natural Gas (LNG) demand as a cleaner marine fuel, but LNG alone cannot meet emission reduction goals. It is considered a transitional fuel until sufficient infrastructure is established, and additional technologies will need to be implemented to limit carbon emissions and meet regulatory requirements. During the transition period, LNG stands out as a fuel capable of reducing CO_2 emissions by 25% compared to low-sulphur marine diesel oil. However, the additional highlight must be addressed to the methane slip effect which appears from the combustion cycle of fuel and processes related to the LNG gas management on the vessels. Methane slip occurs when unburned methane, a potent greenhouse gas, is released into the atmosphere during the fuel combustion cycle. This phenomenon is particularly relevant for engines using LNG as a primary fuel source. Despite LNG's reputation for lower emissions of sulphur oxides (SOx) and nitrogen oxides (NOx) compared to conventional marine fuels, inadvertent methane leakage can undermine its environmental benefits. In 2018, Herdzik J. published the study results of methane slip during cargo operations on LNG carriers and LNG-fueled vessels; it was indicated that the methane leakage level can fluctuate from 1-10%. Methane slip requires a multi-faceted approach that includes both technological advances and operational practices. Engine manufacturers and designers are constantly striving to develop more efficient combustion processes and emission control systems to minimise methane slip and, in parallel, to create an environmentally sustainable infrastructure for LNG fuel during the period when the maritime industry transitions towards zero-emission technologies like hydrogen fuel cells or ammonia propulsion [4].

In order to achieve the decarbonization goals established for the marine shipping sector by the IMO, additional technological progress is needed, and in past years carbon capture and storage and utilization solutions have drawn industries' attention. There are currently a few ways to manage CO_2 as a material: 1) carbon capture, storage and utilization in which the captured CO_2 is converted into other substances via chemical reaction within hydrogen and other substances injection into the process post CO_2 is separated from the flue gases and 2) carbon capture and storage in which way the CO_2 separated from exhaust gases is turned into the liquid or either solid phase and then stored underground [5].

According to the statistics database of the National Energy Technology Laboratory in 2023, close to 400 total CCS projects were registered worldwide. The breakdown of project categories is illustrated in Fig. 1 [6]. The carbon capture technologies implementation in the shipping industry in 2021 was marked by the first project of CO_2 capture machinery implemented on the ship structure. The system has been installed on the bulk carrier Corona Utility, registered under IMO No. 9748021, and the sea trials have been completed within the announcement of the potential system's compatibility with the ship's machinery to perform separation and capture of CO_2 emission from the flue gas generated by engines [7].
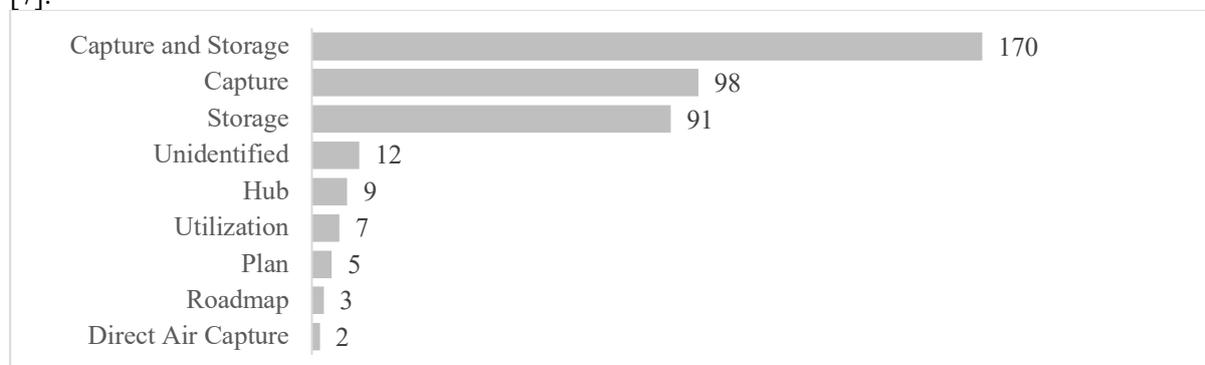

Fig. 1. Carbon capture and storage database as of May 2023 – number of CCS projects worldwide

Although the database primarily contains registered projects for shore-based or offshore-based facilities, it should be noted that shipping also plays a role in CCS-based decarbonization methods. The

application of CCS technologies in the shipping industry was reviewed by the Oil and Gas Climate Initiative in 2021. They published a feasibility study analysing energy balances, fundamental physics, and integration challenges for implementing carbon capture technologies on ship-based structures. The study confirmed that LNG carriers or LNG-fuelled vessels offer the most convenient path to a feasible carbon capture system. The the propulsion type and exhaust gas composition providesufficient waste heat and rest of infrastructure for the liquefaction and storage of captured CO_2 [8]. The comparison table within the criteria of the LNG carrier advantage versus other heavy fuel engine-equipped vessels is presented in Tab. 1.

Table 1

Comparison of different types of vessels for the most convenient option for CCS application

Evaluation criterion	Medium range tanker	Suez-max tanker	LNG carrier
Main engine type	7.2MW 2-stroke	15.7MW 2-stroke	3x3.8MW 4-stroke
Primary fuel	Heavy fuel oil	Heavy fuel oil	Natural gas
Space availability	Yes	Yes	Yes
Exhaust gas heat availability	Average	Poor	Good
Sulphur content/fuel impurities	High	High	Low
Representative of a wider fleet	Yes	Yes	No
Impact of success	High	High	Low

In addition to the comparison of vessels' technical capabilities to adopt carbon capture technologies, carbon capture technologies have to be analyzed in a similar way. In industry, four leading technologies are being indicated as potential for CO_2 capture. Along with the key criteria, the comparison of technologies is presented in Tab. 2. Comparing the presented technologies, the chemical absorption and cryogenic separation methods stand out from the table as the most compatible technologies for CCS.

The cryogenic separation method is compatible with LNG-fuelled vessels such as LNG carriers, but there have been limited studies devoted to considering the LNG fuel/cargo cold potential application for cryogenic CO_2 capture [9]. Moreover, to date, no technical evaluations have been conducted related to floating storage regasification units (FSRUs), which play a significant role in independent energy delivery to regions. FSRUs handle LNG not only as cargo but also in regasification processes, by which the LNG is converted back into the gas phase during the heat exchange process [10].

Table 2

Comparison of different types of carbon capture technologies for CCS application

Capture method/treatment type of exhaust gas			
Criterion	Chemical treatment	Absorption treatment	Membrane treatment	Cryogenic treatment
Maturity	High	Low	Low	Medium
CO_2 purity	99%	Purity and capture rate are linked. In general, CO_2 purity is low (80% for adsorption, 60% for membranes)		99.9%
CO_2 capture rate potential	90-99%			90-99%
Sensitivity to impurities	SOx, NOx	SO_X, NO_X, H_2O	SO_X; NO_X	SO_X, H_2O

The study aims to assess the possibility of utilising LNG's cryogenic cold potential on FSRU-based vessels through the regeneration process of flue gas heat to cool down the exhaust gases while separating H_2O condensate and CO_2 to the liquid phase. Cryogenic carbon capture is a process used to separate CO_2 from post-combustion exhaust gas cycles. The separated CO_2 is typically compressed and then

cooled to a temperature of around -50°C, at which point it condenses into a liquid. The liquid form of CO_2 has a much smaller volume than its gaseous form, making it more practical to transport and store. At a temperature of -50°C, the storage density of liquid CO_2 is approximately 1,156 kg/m^3. This high storage density serves as an advantage for carbon capture and storage (CCS) strategies, such as onboard vessel storage before further utilization. In this research, the energy balance calculation methodology has been adopted to analyse the energy exchange between different fluids involved in the cogeneration cycles of regasification activities, including LNG, R-290 refrigerant, and seawater. Through the local experimental measurements, it has been determined that the exhaust gas temperature from regassification boilers varies around 100°C, while the temperature of exhaust gases from propulsion engines fluctuates around 270°C; temperatures are presented after the exhaust gas passes the economisers. The heat balance calculation methodology allows the identification of potential areas for improvement and the implementation of targeted solutions to enhance the performance of the regasification process while also improving compliance with IMO decarbonization regulations.

2. LIQUEFIED NATURAL GAS REGASIFICATION SYSTEM DESCRIPTION

The FSRU-based vessel considered in this study has a storage capacity of 170,000 m^3 and the capability to perform regasification of roughly 17,000 m^3 LNG per day. The regasification unit is equipped with both open-loop and closed-loop regasification performance capabilities.

During the open-loop regime, sufficient temperature seawater is used to heat the heat transfer fluid (R-290), which is then used to transfer heat to the LNG through several heat exchangers, thus converting the liquid gas into the gas phase. During the open-loop regime cycle, starting from approx. -160°C at three stages LNG is being heated to the natural gas phase temperature of approx. +13°C:

- In the first regasification stage, the regasification pumps submerged in LNG of the cargo tank transfer cargo to the suction drum at 5 bar pressure (absolute), during the transfer the LNG temperature is -155°C.
- From the suction drum, the LNG is distributed to LNG vaporisers. The considered FSRU is equipped with 3 individual LNG vaporisers.
- On the way to the LNG vaporiser, the LNG passes the BOG recondenser. At this stage, the LNG is heated up to approximately -150°C;
- After the BOG recondenser, the LNG enters the LNG vaporiser. At this stage, the LNG is heated up to approximately -30°C (LNG is converted into vapour).
- In the third step, gas already in the vapour phase enters the trim heater, where it is heated up to approximately 10°C and then delivered to the gas grid for consumers. The LNG regasification cycle is presented in the scheme below.

At the LNG vaporiser and trim heater stages, the gasses are in contact with heat transfer fluid (R-290), which is heated up by the sea water to a sufficient temperature to contact with the gas. In the open-loop cycle, the sea water. temperature is sufficient to heat R-290. In the cold temperature season, when the sea water. temperature drops below 10°C, the steam has to be injected into the regasification system to heat the sea water. to 17-19°C. In such a way, we can state that the regasification cycle is based on heat exchange between three individual fluids: the sea water cycle, the R-290 cycle, and the LNG cycle. In 2021, Naveiro et al. [11] published research on environmental measures applicable to floating storage regasification units, which indicated that considering the environmental perspective, open-loop operations in ports must be permitted by the environmental agency, requiring an environmental impact assessment due to the potential environmental consequences associated with marine ecosystems. The intake and discharge of seawater during open-loop regasification operations can result in the entrainment and impingement of marine organisms against intake screens and other infrastructure. Due to the potential negative operational exposure to the environment, open-loop operations are assessed on a case-by-case basis.
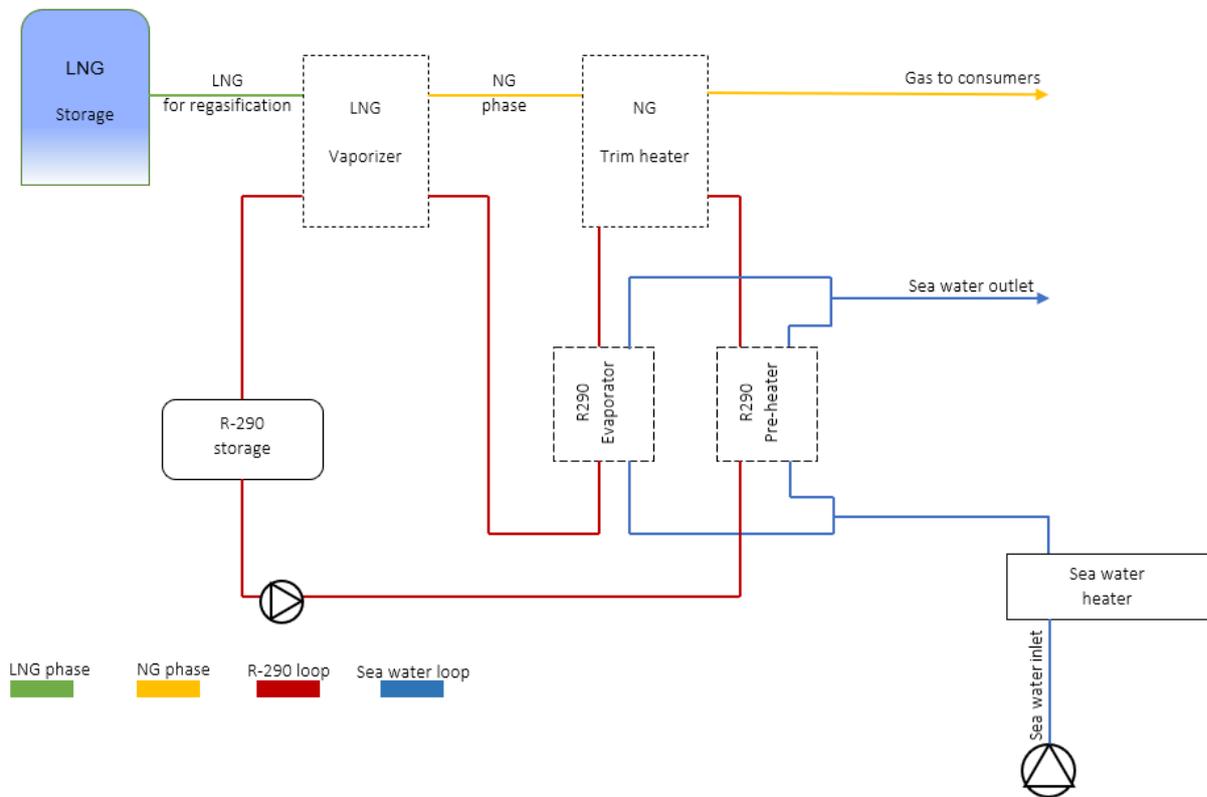
Fig. 2. Regasification cycle on the FSRU-based vessel

3. HEAT BALANCE ANALYSIS OF THE LNG REGASIFICATION PROCESS

The regasification process comprises a series of thermodynamic heat exchange processes between liquid fluids and gas-phase heating fluids. Several formulas practically can be applied in order to estimate heating balance as a method for identifying the thermodynamic exchanges [12].

$$Q = M * Cp * \Delta T, \tag{1}$$

where: M – flow rate in mass units, kg/s; C_p – specific heat capacity; ΔT – temperature difference of fluid inlet and outlet.

Equation (1) represents the formula for determining the quantity of heat, denoted as Q, needed to change the temperature of a substance of mass M by temperature difference ΔT, considering the specific heat capacity Cp of the substance. The specific heat capacity is the amount of heat required to raise the temperature of one unit of mass of the substance by one degree Celsius. The formula can be used to estimate fluids' heat balance after the heat exchange in the fluid remains in the same phase.

$$Q = ((M * (h_1) - \left(C_p(t * M)\right), \tag{2}$$

where: h_1 – enthalpy of fluid (fluid inlet condition); t – temperature of fluid (outlet temperature), °C.

Equation (2) is employed to ascertain the amount of heat necessary for elevating the temperature of a substance from its initial state of h_1 to a final temperature of t. In the equation, Q represents the amount of heat required, M represents the mass of the substance being heated, C_p represents the specific heat capacity of the substance, h_1 represents the initial temperature of the substance, and t represents the final temperature of the substance. The specific heat capacity, C_p, is a property of the substance that describes how much heat energy is needed to raise the temperature of one unit of mass of the substance by one degree Celsius or Kelvin. The equation is commonly used in thermodynamics and heat transfer applications to determine the energy required for a heating process [13].

$$Q = (M(h_2 - h_1))_{\text{subcooled liquid}} + (M(h_3 - h_2))_{\text{two-phase}} + (M(h_4 - h_3))_{\text{superheated vapour}}, \quad (3)$$

Equation (3) is used to calculate the amount of energy Q required for a substance with a mass of M to change its state from a lower enthalpy h_1 to a higher enthalpy h_2 while undergoing a temperature change of $\triangle$ T. The term $M(C_p \triangle T)$ represents the amount of energy required to change the temperature of the substance, where C_p is the specific heat capacity of the substance. The term $M(h_2 - h_1)$ represents the energy required for the substance to change its state from h_1 to h_2. The term $M(\triangle h)$ represents any additional energy required due to the specific conditions of the process, such as changes in pressure or volume.

4. HEAT BALANCE CALCULATION IN THE LNG REGASIFICATION CYCLE

As a starting point, the steam heaters' performance of heat balance is calculated. It is necessary to calculate the heat being entered into the system as the steam and then subtract the heat remaining in the steam condensate after the heat exchange on the exit of the heater to calculate the heat transfer of the heater. The calculation of heat energy can be determined using the following equations: (4) – steam side; (5) – seawater side.

$$\text{Heat transferred} = \text{Heat in} - \text{Heat out}$$

$$Q_{\text{Steam side}} = ((M* (h_1) - (C_p(t*M)), \quad (4)$$

$$Q_{\text{Steam side}} = 41045 * ((2718) - (4.20 * 80) = 27,170 \text{ kW},$$

where: h_1 = 2718 kJ/kg (enthalpy of steam at 120.9°C and 1.0 bar); C_p = 4.20 kJ/kg°C (specific heat of water kJ/kg°C); M = 41,045 kg/hour (steam flow rate).

$$Q_{\text{Seawater side}} = (M* (h_2 - h_1), \quad (5)$$

$$Q_{\text{Seawater side}} = M* (h_2 - h_1) = 1,221,652 * (105.38 - 25.818) = 26,999 \text{ kW},$$

where: h_2 = 25.818 kJ/kg (enthalpy of seawater at 25°C and 6.0 bar); h_1 = 105.38 kJ/kg (enthalpy of seawater at 25°C and 6.0 bar); M = 1,221,652 kg/hour (mass of steam flow rate).

The heated seawater is then directed to the R-290 preheater. The calculation of the heat energy is conducted using the subsequent formulas: (6) – R-290 side of the preheater; (7) – seawater side of the preheater.

$$Q = M * Cp * \triangle T, \quad (6)$$

$$Q_{\text{R-290 side}} = 276,000 * 2.456 * 31 = 5,837 \text{ kW},$$

where: M = 276,000 kg/hour (flow of R-290); Cp = 2.456 kJ/kg°C (specific heat of R-290 [14]); $\triangle$ T = 31°C.

$$Q_{\text{seawater side}} = 718515 * 4.20 * 7.4 = 6,173 \text{ kW}, \quad (7)$$

where: M = 718,515 kg/hour (seawater flow rate); Cp = 4.20 kJ/kg°C (specific heat of seawater); $\triangle$ T = 7.4°C.

After the preheater, R-290 is directed to the LNG trim heater. The following equations estimate the heat exchange at the LNG trim heater: (8) – for the R-290 side of the trim heater; (9) – for the LNG side of the trim heater.

$$Q = M * Cp * \triangle T, \quad (8)$$

$$Q_{\text{R-290 side}} = 276,000* 2.456 * 18.77 = 3,329 \text{ kW},$$

where: M = 276,000 kg/hour (R-290 flow rate); Cp = 2.456 kJ/kg°C (specific heat of R-290); $\triangle$ T = 18.77°C (temperature change of R-290).

$$Q_{\text{NG}} = (M* (h_2 - h_1), \quad (9)$$

$$Q_{\text{NG}} = M* (h_2 - h_1) = 84,000 * ((-50) - (-191)) = 3,290 \text{ kW}.$$

where: h_2 = -191 kJ/kg (enthalpy of methane at 14.7°C and 4.96 MPa); h_1 = -50 kJ/kg (enthalpy of methane at -37.5°C and 51.9 bar; M = 84,000 kg/hour (methane gas flow rate).

At the trim heater, R-290 is directed to the R-290 evaporator. The following equations estimate the heat exchange at the R-290 evaporator: (10) – for the R-290 side of the evaporator; (11) – for the seawater side of the evaporator.

$$Q = ((M* (h_1) - (C_p(t*M)), \quad (10)$$

$$Q_{R-290\ side} = 260,000 * ((198.25) - (1.7729 * 11.2)) = 12,883\ kW$$

where: h_1 = 198.25 kJ/kg (enthalpy of R-290 at -0.73°C and 5.92 bar); C_p = 1.7729 kJ/kg (specific heat of R-290 at 11.2°C and 54.6 bar); M = 260000 kg/hour (R-290 flow rate).

$$Q = M * C_p * \triangle T, \qquad (11)$$
$$Q_{seawater\ side} = 2,441,236 * 4.20 * 4.7 = 13,322\ kW,$$

After R-290 is heated, it flows to the LNG vaporiser. Estimations of heat balance are presented in the following equations: (12) – for the R-290 side of the LNG vaporiser; (13) – for the LNG side of the LNG vaporiser.

$$Q = (M(h_1 - h_2))_{superheated\ vapour} + (M(h_2 - h_3))_{two-phase}, \qquad (12)$$
$$Q_{R-290\ side} = (276,000 * (592.72 - 581.72)) + (276,000 * (581.72 - 208.33)) = 29,466\ kW.$$

where: M = 276,000 kg/hour (R-290 flow rate); h_1 = 592.68 kJ/kg (enthalpy of R-290 at 11.22°C and 5.19 bar); h_2 = 581.72 kJ/kg (enthalpy of R-290 at 5°C and 5.19 bar); h_3 = 581.72 kJ/kg (enthalpy of R-290 at 5°C and 5.19 bar).

$$Q = (M(h_2 - h_1))_{subcooled\ liquid} + (M(h_3 - h_2))_{two-phase} + (M(h_4 - h_3))_{superheated\ vapour}, \qquad (13)$$
$$Q_{LNG} = (122,573(-635 + 870)) + (122,573(-370 + 635)) + (122,573(-191 + 370)) =$$
$$= 23,118\ kW.$$

where: M = 122573 kg/hour (LNG flow rate); h_2 = -635 kJ/kg (enthalpy of methane vapour at -96°C and 53.3 bar); h_1 = -870 kJ/kg (enthalpy of methane at -150.10°C and 53.3 bar); h_3 = -370 kJ/kg (enthalpy of methane vapour at -96°C and 53.3 bar); h_4 = -191 kJ/kg (enthalpy of methane at -37.5°C and 51.9 bar).

Table 3

Summary of energy balance results at the heat exchangers

Seawater Steam Heater		R-290 Preheater		Trim Heater		R-290 Evaporator		LNG Vaporiser	
Seawater steam	Seawater	Seawater	R-290	R-290	Natural gas	R-290	Seawater	R-290	LNG
27,170	26,999	6,173	5,837	3,329	3,290	12,883	13,322	29,466	23,118
Energy conversion efficiency ratios (η):									
0.99		0.95		0.98		0.97		0.78	

5. THE COLD POTENTIAL OF LNG FOR CO₂ CAPTURE

The general idea of cryogenic carbon capture is to reduce CO_2 emissions by extracting carbon dioxide from exhaust gases, converting it into a liquid phase or solid phase (dry ice), and then storing and disposing of it.

Cold potential of LNG. The LNG regasification process on FSRU or LNG/C (LNG carrier) type vessels, requires regasification and heating through heat supply. The concept of using the LNG regasification system is based on the concept of passing the LNG through the heat exchanger where the exhaust gas is cooled by the LNG and the heat of the exhaust gas is transferred to the LNG where the LNG acts as a dividing element for separation of carbon dioxide from the exhaust gas. Fig. 3 illustrates the process of CO_2 separation from exhaust gases and the CO_2 phase diagram across wide ranges of pressures and temperatures [15]:

1. The first stage is exhaust gas drying. The exhaust gases need to be cooled down to a temperature 20 of °C in order to remove H_2O from the exhaust gases. At a temperature of 0°C, the H_2O condenses so then can be separated.

2. Te second stage is liquefaction. After the H_2O as a condensate is removed from the flue gases, in the next stage, the CO_2 is cooled further to achieve a liquid phase. In general, within a temperature range between -56.6°C and 31°C and a pressure range of greater than 5.2 bar (abs) and less than 74 bar (abs), CO_2 is in a liquid phase [16]. The captured CO_2 can be stored in carbon

capture emission tanks and, due to density parameters, is 1032 kg/m³ in liquid form and 1562 kg/m³ in solid form.
3. The third stage is the build-up of pressure.   During the cooling down stage, it is necessary to build up pressure to create an environment conducive to liquid phase formation.
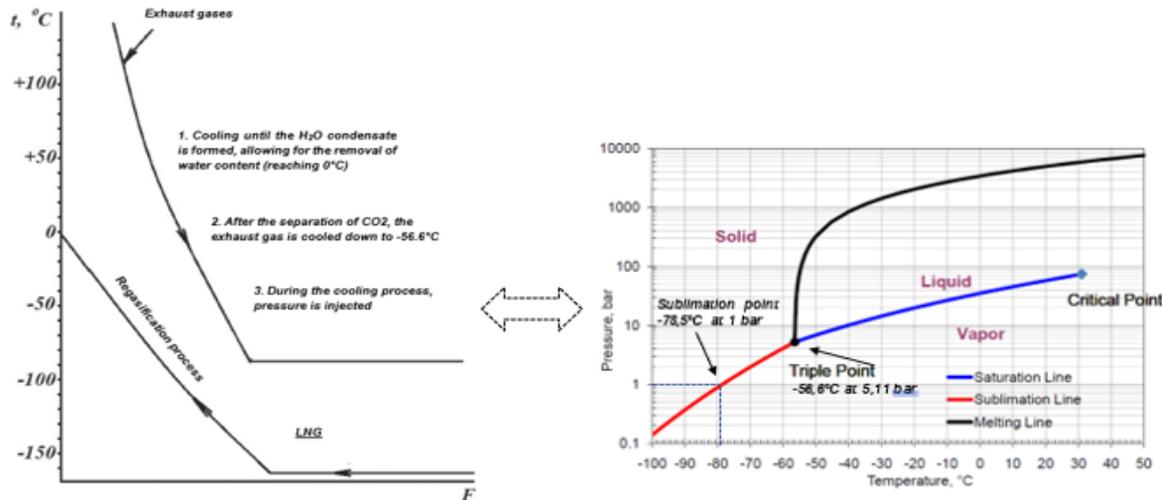

Fig. 3. LNG cold potential utilisation – CO_2 phase diagram

The separation and exchange of heat/cold potentials between gases require a sufficient energy indication. The amount of energy required to be transferred from the LNG to lower the exhaust gas temperature to the phase change threshold is critical. As the exhaust gas temperature decreases, the LNG absorbs heat, which is utilized in the regasification process. The evaluation can be made based on the scheme illustrated in Fig. 4.
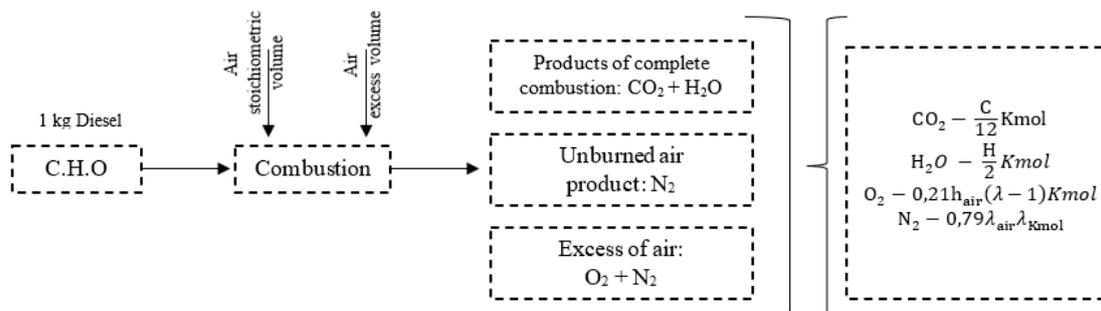

Fig. 4. Combustion cycle considering diesel as a fuel

The main composition of marine diesel oil consists of carbon, hydrogen and oxygen. The composition of 1 kg of diesel equals 0.87 kg – carbon, 0.12 kg – hydrogen and 0.01 kg – oxygen. The combustion of carbon produces carbon dioxide ($C+O_2 = CO_2$), where the atomic mass of carbon is 12 kg/kmol and the molecular weight of oxygen is 32 kg/kmol. The reaction of 1 kg carbon oxidation to carbon dioxide in mass units can be expressed as presented on the left side of Tab. 4. From the equations of the combustion process, the equation can be expressed to determine the necessary amount of oxygen for the oxidation of 1 kg fuel (composition C, H, O). Afterwards, the equation is expressed to indicate the air excess for the necessary volumetric of air – L_{air}. The result is illustrated on the table's right side.

During the diesel fuel combustion cycle, oxidation generates an exhaust gas consisting of CO_2, H_2O, O_2 and N_2. A combustion rule to be noted is as follows: if the necessary volume of air expressed in stoichiometric conditions would be injected in the combustion process of a four-stroke engine, the

injected diesel fuel would not burn completely due to non-stoichiometric conditions; for this reason, the excess of air (λ) has to be injected into the combustion process. Accordingly, Equation (14) can be expressed to indicate the nitrogen emission on exhaust gases after 1 kg of diesel fuel combustion. The volumetric composition of exhaust gases presented is illustrated in Fig. 4.

$$O_2 = 0.21L_{air}(\lambda - 1), \tag{14}$$

$$N_2 = N_{combusted\ air} - N_{air\ excess},$$

$$N_2 = 0.79L_{air} + 0.79L_{air}(\lambda - 1) = 0.79L_{air}(1 + \lambda - 1) = 0.79L_{air}\lambda,$$

Once the volumes have been determined, the next step is to determine the specific heat to measure the energy required to condense and separate H_2O from the flue gas. Equation (15) is then used in the subsequent cooling stage to liquefy the CO_2.

$$C_p(CO_2 + H_2O + O_2 + N_2), \tag{15}$$

$$C_p = C_v + R,$$

where: C_p – the specific heat capacity at constant pressure, which is the energy required to raise the temperature of a substance by one degree Celsius while maintaining a constant pressure, J/g°C or J/mol°C units; C_v – the specific heat capacity at constant volume is the energy required to raise the temperature of a substance by one degree Celsius while maintaining its volume, J/g°C or J/mol°C units and interpolation of figures is presented in table (Tab. 5); R – gas constant, 8,314 kJ/kmol°C.

Table 4

Diesel combustion reaction and equation of air amount necessary for the process

1. Combustion process	a) Stoichiometric conditions:	2. The necessary amount of air for the of 1 kg fuel oxidation (stoichiometric conditions)

1. Combustion process

$$C + O_2 = CO_2$$
$$1Kmol\ C + 1kmol\ O_2 = 1kmol$$
$$1kg\ C + \frac{1}{12}kmol\ O_2 = \frac{1}{12}kmol\ CO_2$$
$$Ckg\ C + \boxed{\frac{C}{12}\ kmol\ O_2} = \frac{C}{12}kmol\ CO_2$$

$$4H + O_2 = 2H_2O$$
$$4kmol\ H + 1kmol\ O_2 = 2kmol\ H_2O$$
$$1kmol\ H + \frac{1}{4}kmol\ O_2 = \frac{2}{4}kmol\ H_2O$$
$$1kg\ H + \frac{1}{4}kmol\ O_2 = \frac{2}{4}kmol\ H_2O$$
$$Hkg\ H + \boxed{\frac{H}{4}\ kmolO_2} = \frac{2H}{4}kmol\ H_2O$$

$$1kmol\ O_2 - 1kmol\ O_2 = 0$$
$$1kg\ O_2 - \frac{1}{32}kmol\ O_2$$
$$0 - \boxed{\frac{0}{32}\ kmol\ O_2} = 0$$

a) Stoichiometric conditions:

Necessary amount of air for the oxidation of 1 kg of fuel composition C-H-O:

$$M_{O_2} = \boxed{\left[\frac{C}{12} + \frac{H}{4} - \frac{0}{32}\right]}kmol\ O_2/1kg\ fuel$$

$$L_{air} = \frac{1}{0,21}\left[\frac{C}{12} + \frac{H}{4} - \frac{0}{32}\right]kmol\ air/1kg\ fuel$$

Where, L_{air} – stoichiometric constant, Kmol O_2/1kg fuel.
Volumetric composition of air: O2 = 21%; N2 = 79%

b) Non-stoichiometric conditions

$$\lambda = \frac{L_{actual}}{L_{stoichiometric}}$$

As the R is a constant figure, for the mixture of exhaust gases, the specific heat capacity at constant volume has to be calculated based on Equation (16). The equation is derived by summing the elemental compositions (where the specific heat by volume of each element is multiplied by its molar content and divided by the total number of moles).

$$C_{v(mixture)} = \sum_{i=1}^{n} c_{v(i)} * r_i; \quad r_i = \frac{M_i}{\sum_{i=1}^{n} M}, \tag{16}$$

$$r_{CO_2} = \frac{\frac{C}{12}}{\left(\frac{C}{12} + \frac{H}{2} + 0,21L_{air}(\lambda - 1) + 0,79L_{air}\lambda\right)},$$

$$L_{air\ (1kg\ diesel\ fuel)} = \frac{1}{0,21}\left(\frac{C}{12} + \frac{H}{4} - \frac{0}{32}\right) = \frac{1}{0,21}\left(\frac{0.87}{12} + \frac{0.12}{4} - \frac{0.01}{32}\right) = 0.490\ kmol,$$

$$r_{CO_2} = \frac{\frac{C}{12}}{\left(\frac{C}{12} + \frac{H}{2} + 0,21L_{air}(\lambda - 1) + 0,79L_{air}\lambda\right)},$$

$$r_{H_2O} = \frac{M_{H_2O}}{\left(\frac{C}{12} + \frac{H}{2} + 0,21L_{air}(\lambda - 1) + 0,79L_{air}\lambda\right)} \leftarrow calculated\ individualy\ for\ each\ element,$$

$$C_v + R = C_{p\ (mixture)} \leftarrow at\ the\ end, the\ specific\ heat\ capasity\ can\ be\ calculated,$$

$$Q = C_p\ \Delta\ t, kJ,$$

Table 5

The interpolation of molar heat capacities of gas at constant volume at different temperature intervals

Gas type	Mc_v, kJ/kmol°C	
	0-1,500°C	1,501–2,800°C
Air	20.600+0.002638·t	22.387+0.001449·t
Oxygen O_2	20.930+0,004641·t − 0.00000084·t²	23.723+0.001550·t
Nitrogen N_2	20.398+0.002500·t	23.723+0.001457·t
Hydrogen H_2	20.684+0.000206+0.000000588·t²	19.678+0.001758·t
Carbon oxide CO	20.597+0.002670·t	22.490+0.001430·t
Carbon dioxide CO_2	27.941+0.019·t – 0.000005487·t²	39.123+0.003349·t
Water H_2O	24.953+0.005359·t	26.670+0.004438·t

6. CONCLUSIONS

In recent times, there has been a growing emphasis on managing the adverse effects of technology. To achieve decarbonization objectives, the maritime transportation industry has implemented various regulations that aim to compel ship owners to adopt alternative fuels for their vessels. The growing demand for LNG as a transition fuel towards decarbonization goals has highlighted its role in the energy transition. However, it also underscores the necessity for implementing additional technologies on vessels. These advancements are crucial to achieve a 70% reduction in carbon emissions by 2050, in line with the IMO's objectives.. According to the CCS projects database, as of May 2023, almost 400 projects have been registered worldwide that are linked to the utilization of captured CO_2 emissions. In the marine sector, the cryogenic carbon capture technology on LNG-fuelled vessels stands out as a potential solution to separate and capture CO_2 from the exhaust gases. However, to this day, such technology has not been integrated into vessels and this indicates limited research on cryogenic carbon capture technology implementation on the vessel. The FSRU vessel, which can convert LNG (liquefied natural gas) into natural gas through various heat exchange processes, undergoes heat balance with varying capacities for each phase. These capacities are as follows: steam heater (26,999 kW), R-290 preheater (5,837 kW), trim heater (3,290 kW), R-290 evaporator (13,322 kW) and LNG vaporiser (23,118 kW). The cryogenic carbon capture process utilizes the cryogenic temperature of LNG, which allows the achievement of two objectives: reducing exhaust gas temperature and providing heat absorption for regasification processes. The low temperature plays a crucial role in separating carbon dioxide in subsequent cycles. These cycles are as follows: 1) lowering the flue gas temperature to the point of H_2O condensation, 2) separating H_2O from the flue gases and 3) further reducing flue gas temperature to enable CO_2 liquefaction. The temperature is aligned with the pressure and requires an increase in pressure in order to achieve liquefaction conditions. Mathematical modelling is employed for heat energy calculations in this research. The next stage of this study aims to determine the amount of energy required for CO_2 capture.

References

1. Hua, W. & Sha, Y. & Zhang, X. Research progress of carbon capture and storage (CCS) technology based on the shipping industry. *Ocean Engineering*. 2023. Vol. 281. No. 114929.
2. Chua, Y. & Soudagar, I. & Ng, S. & Meng, Q. Impact analysis of environmental policies on shipping fleet planning under demand uncertainty. *Transportation Research Part D: Transport and Environment*. 2023. Vol. 120.
3. Wang, S. & Zhen, L. & Psaraftis, H. & Yan, R. Implications of the EU's inclusion of maritime transport in the emissions trading system for shipping companies. *Engineering*. 2021. Vol. 7. No. 5. P. 554-557.
4. Herdzik, J. Methane slip during cargo operations on LNG carriers and LNG-fueled vessels. *New Trends in Production Engineering*. 2018. Vol. 1. P. 293-299.
5. Kawai, E. & Ozawa, A. & Leibowicz, B. Role of carbon capture and utilization (CCU) for decarbonization of industrial sector: A case study of Japan. *Applied Energy*. 2022. Vol. 328. No. 120183.
6. *National Energy Technology Laboratory. Carbon Capture and Storage Database*. Available at: https://netl.doe.gov/carbon-management/carbon-storage/worldwide-ccs-database.
7. *Kawasaki Kisen Kaisha. World's First CO_2 Capture Plant on Vessel Installed on Coal Carrier CORONA UTILITY Launch of the CC-OCEAN Project Demonstration*. 2021. Available at: https://www.kline.co.jp/en/news/csr/csr7601431474845700352/main/0/link/210805EN.pdf.
8. Organization of Oil and Gas Climate Initiative. *Is Carbon Capture on Ships Feasible?* 2021. Available at: https://safety4sea.com/wp-content/uploads/2021/11/OGCI-STENA-Is-carbon-storage-technically-feasible-2021_11.pdf.
9. Baxter, L. & Baxter, A. & Burt, S. *Cryogenic CO_2 Capture as a Cost-Effective CO_2 Capture Process*. Environmental Science, Engineering. 2009.
10. Cann, D. & Willson, P. & Font-Palma, C. Experimental exploration of cryogenic CO_2 capture utilising a moving bed. *14th Greenhouse Gas Control Technologies Conference Melbourne 21-26 October 2018 (GHGT-14)*. Available at: https://papers.ssrn.com/sol3/papers.cfm?abstract_id=3366196.
11. Naveiro, M. & Gomez, M. & Fernandez, I. & Insua, A. Energy efficiency and environmental measures for floating storage regasification units. *Journal of Natural Gas Science and Engineering*. 2021. Vol. 96. No. 104271.
12. Martinaitis, V. & Vegytė, N. & Paulauskaitė, S. & Šakmanas, A. *Techninė termodinamika ir šilumokaita*. 2005. Available at: https://www.mokslobaze.lt/termodinamikos-ir-silumokaitos-konspektas-egzui.html [In Lithuanian: *Technical thermodynamics and heat exchange*].
13. Merker, G.P. & Schwarz, C. & Stiesch, G. & Otto, F. *Simulating Combustion – Simulation of combustion and pollutant formation for engine-development*. New York: Springer. 2004.
14. *National Refrigerants. Safety Data Sheet of R290 Propane*. 2021. Available at: https://refrigerants.com/wp-content/uploads/2019/12/SDS-R290-Propane.pdf.
15. Bezyukov, K. Uses of a hladopotentsial of the liquefied natural gas for decrease in emissions of carbon dioxide heat power installations. *Ship Power Plants Syst. Devices*. 2016. DOI: 10.21821/2309-5180-2016-7-3-143-155.
16. *Linde. Safety advice – Carbon Dioxide*. Available at: https://www.linde-gas.com/en/images/LMB_Safety%20Advice_01_66881_tcm17-165650.pdf.